Modulator-Free Green Synthesis of the Calcium-Terephthalate Metal-Organic Framework Derived from Waste Eggshells

Gizelle R. van Niekerk, Henrietta W. Langmi[*]

Department of Chemistry, University of Pretoria, Private Bag X20, Hatfield 0028, South Africa

ABSTRACT

Conventionally, the four-component calcium-terephthalate (Ca-BDC) metal–organic framework (MOF), $Ca(BDC)(DMF)(H_2O)$, has been synthesized from commercial calcium nitrate $(Ca(NO_3)_2)$ and calcium carbonate $(CaCO_3)$, which in turn are manufactured from naturally-occurring minerals by energy-intensive processes. This study presents a primary investigation on the modulator-free solvothermal synthesis of $Ca(BDC)(DMF)(H_2O)$ derived from waste eggshells as green precursors. $Ca(BDC)(DMF)(H_2O)$ crystallizes as two possible phases, namely the triclinic (Ca-BDC-tric) and orthorhombic (Ca-BDC-orth) phase. This study presents an in-depth investigation on the influence of reaction temperature and solvent volumes on eggshell-derived $Ca(BDC)(DMF)(H_2O)$ product phase. Investigations were conducted at long reaction times to ensure complete reaction of green eggshell precursors. Low water (H_2O) and high N,N-dimethylformamide (DMF) volumes were found to inhibit solvothermal synthesis. 7.6 mL H_2O was determined to be the minimum H_2O volume threshold for successful Ca-BDC-tric synthesis, above which further increasing the H_2O volume produced porous Ca-BDC-tric at higher yield, which proved favorable due to reduction of toxic DMF. Ca-BDC-orth and Ca-BDC-tric were obtained at 150 °C and 110 °C respectively, whereas dual-formation of both phases prevailed at 130 °C, thereby informing the rough temperature range at which Ca-BDC-tric morphs into Ca-BDC-orth. Ultimately, this study introduces a green solvothermal method for valorizing eggshell waste into value-added $Ca(BDC)(DMF)(H_2O)$ for sustainable eggshell waste management and alleviation of environmental health concerns associated with eggshell disposal.

1. Introduction

As estimated in the 2021 Food Waste Index Report, a global 1.3 billion tons of food waste is generated annually, with a contribution of 61% by households and 26% by food industries [1]. According to the United Nations Environment Programme (UNEP), almost half of discarded food waste is inedible and presents an unharvested resource with high potential for conversion into value-added biomaterials [1]. Waste eggshells are an example of such a resource where egg production and, thus, eggshell waste generation has increased by 150% over the past 30 years [2]. Leading egg producers are China, India and the USA which produce an annual 458, 109 and 95 billion eggs, respectively [2]. In 2019 alone, China produced 24.8 billion kilograms of eggshells, equivalent to half the global eggshell mass generated annually, thereby exemplifying how prolific eggshells are as a potential resource [2]. Eggshells constitute 9–12% of total egg mass and are composed of 98% dry matter and 2% water (H_2O) [3]. Eggshells are rich in calcium carbonate $(CaCO_3)$ which makes up 94% of eggshell mass and is intertwined with calcium phosphate and magnesium carbonate to form a fibrous-protein organic matrix [4]. Micro-nutrients are present at trace quantities in eggshells, namely iron, copper, sulfur, boron, silicon and zinc [3]. However, disposal of waste eggshells presents a major challenge because decay of the protein-rich organic membrane attracts rats and causes fungal growth on eggshells that stimulates the proliferation of pathogens [5]. For these reasons, it is crucial that eggshells be disposed of in sanitary landfills with proper gas and leachate management. However, sanitary landfills require immense financial input and manpower, oftentimes only being effectively operational in developed countries [6]. Therefore, food waste, especially in developing nations, ultimately ends up in uncontrolled, open dumps where toxic drainage contaminates soil and groundwater [6,7]. Hence, the Environmental Protection Agency ranked eggshell waste as the 15th major pollution problem stemming from the food industry, making it imperative to recycle waste eggshells [8].

Several methods exist for the valorization of waste eggshells and, therefore, eggshell-based products have a variety of applications in the

* Corresponding author.
E-mail address: henrietta.langmi@up.ac.za (H.W. Langmi).

medical, dental, commercial and industrial fields. Eggshell powder was determined to be an effective polishing agent for reducing surface roughness of dental plates [9]. Calcium supplements have been created from eggshell $CaCO_3$ instead of from synthetic $CaCO_3$ derived from oyster shell calcium [10]. Eggshells are utilized as a calcium source in orthopedics from which hydroxyapatite is synthesized for use as a bone graft substitute [11]. The bioavailability of calcium in milk tablets synthesized from eggshell $CaCO_3$ exceeded that of tablets produced from commercial calcium [12]. Heavy metals and toxic hexavalent chromium have been removed from H_2O using eggshells as a sorptive agent [13]. Eggshells are effective neutralizers of highly acidic acid mine drainage, providing an economical alternative to the use of limestone [14].

Metal-organic frameworks (MOFs) are crystalline coordination polymers formed by the three-dimensional assembly of multidentate organic linkers and inorganic metal-containing clusters [15]. MOFs exhibit highly predictable structural frameworks where desired pore diameters and pore volumes can be achieved by adjusting the MOF's metal oxide and varying the length of its organic linker [15]. MOFs with calcium metal centers (Ca-MOFs) boast several advantages over those with transition metal centers. Firstly, calcium is an electropositive element that forms strong ionic bonds with organic ligands in Ca-MOFs, thereby promoting high thermal stability [16]. Secondly, calcium is an earth-abundant metal that constitutes 3.4% of Earth's crust [16]. Consequently, the calcium reagent is easy to source, making Ca-MOF syntheses relatively inexpensive. Thirdly, calcium is a non-toxic reagent and, thus, Ca-MOF syntheses operate in the realm of green chemistry [16]. Lastly, calcium is a lightweight metal that, hence, offers ideally low gravimetric properties [16]. Ca-MOFs have been reported to have potential applications in gas adsorption and separation, catalysis, drug delivery, sensing, and electronics [15].

The four-component calcium-terephthalate (Ca-BDC) MOF, with the formula Ca(BDC)(DMF)(H2O), exists as two possible phases, the high-temperature orthorhombic phase (Ca-BDC-orth) and the low-temperature triclinic phase (Ca-BDC-tric), which was found to be porous [17]. Chang *et al.* determined the mechanism of orthorhombic rod formation, where Ca^{2+} reacts with deprotonated terephthalic acid/ 1,4-benzenedicarboxylic acid ($HBDC^-$) to form Ca-BDC monomers [18]. Thereafter, nucleation of Ca-BDC monomers produces embryonic Ca-BDC, visible as a sheet-morphology [18]. Individual, lone-standing sheets begin to stack immediately once formed by monoclinic crystal growth in the (0 2 0) direction to generate fully-formed orthorhombic rods [18].

MOFs can be generated using one of several known synthetic procedures. Microwave-assisted, mechanochemical and sonochemical syntheses are rapid but produce crystals that are too small for single-crystal X-ray diffraction (SCXRD) [16]. Conversely, solvothermal and hydrothermal syntheses are time-consuming but offer sufficiently large crystals for SCXRD [16].

Mazaj and Logar [17], as well as Jamil *et al.* [19] synthesized the four-component Ca(BDC)(DMF)(H2O) MOF from commercially available calcium nitrate (Ca(NO3)2) and $CaCO_3$ respectively, which, in turn, are manufactured from limestone, dolomite and aragonite using energy-intensive processes [16]. Recent studies exploited eggshells as a calcium source in the mechanochemical and hydrothermal synthesis of three-component Ca(BDC)(H2O)3 in which an ethylene glycol modulator was employed [20]. Conversely, this study performed a modulator-free solvothermal synthesis of four-component Ca(BDC)(DMF)(H2O) from waste eggshells. In doing so, this study improved atom economy by elimination of a modulator and introduced a green method for recycling waste eggshells into value-added Ca(BDC)(DMF)(H2O) for integrated waste management. This study performed an in-depth phase investigation by evaluating the influence of solvent volumes and reaction temperature on product phase at long reaction times to ensure complete reaction of eggshell precursors.

2. Experimental

2.1. Materials

Acetone (99.5%, Sigma-Aldrich); Hydrochloric acid (HCl, 98%, Sigma-Aldrich); N,N-dimethylformamide (DMF, 99%, Radchem); phenolphthalein (99%, LabChem); sodium hydroxide (NaOH, 98%, Sigma-Aldrich); 1,4-benzenedicarboxylic acid (BDC, 98%, Sigma-Aldrich).

2.2. Eggshell powder preparation

Free-range eggshells were cracked open and their internal organic contents were decanted, whereafter their inner-membrane was peeled off. Eggshells were washed in acetone, oven-dried for 30 min at 100 °C and ground into a fine light-pink powder. A back titration was performed to quantify the $CaCO_3$ content of eggshells using 1.0 g eggshells, excess 10.2 M HCl, 0.5 M NaOH and phenolphthalein indicator.

2.3. Eggshell-derived Ca(BDC)(DMF)(H₂O) synthesis

Titration results indicated that $CaCO_3$ constituted 94.92% of eggshell mass. A 50 mL autoclave was utilized at 75% volume capacity to accommodate gas release during oven-heating and prevent excessive pressure build-up· dH2O was added to 0.3824 g of eggshell powder and stirred at 25 °C for 1 h. DMF was added to 0.6838 g of BDC and stirred at 65 °C for 15 min. Solvent volumes investigated are provided in Table 1. The eggshell-H2O solution and BDC-DMF solution were combined and stirred at 65 °C for 15 min. The final mixture was transferred to a 50 mL teflon-lined stainless steel autoclave, which was placed in the oven for the selected time and temperature, Table 1. Thereafter, the autoclave was removed and allowed to cool to room temperature. The solid product was vacuum filtered to remove liquid residue and oven-dried for 8 h at 110 °C.

2.4. Eggshell-derived Ca(BDC)(DMF)(H₂O) characterization

Powder X-ray diffraction (PXRD) was performed using Bruker's D2 Phaser model diffractometer equipped with a Cu-tube x-ray source and Lynxeye detector operated in one-dimensional mode. A 30 kV operating voltage was employed in conjunction with a 10 mA operating current where samples were subjected to a 2θ-scan range of 5°-55° and scan rate of 2 *sec* per 0.05° scan increment. Fourier transform infrared (FTIR) spectra were obtained using Bruker's ALPHA Platinum-ATR model spectrometer and manipulated using OPUS software. Spectra were collected using a 400 cm^{-1} minimum and 4000 cm^{-1} maximum wavenumber setting. Scanning electron microscopy (SEM) images were captured by Zeiss's Gemini Ultra Plus model microscope using a 2.3–2.7 mm working diameter. The extra-high tension setting was activated by applying 1.00 kV of electron accelerating potential between the scanning tip and sample surface. Thermogravimetric analysis (TGA) was performed using the SDT Q600 Analyzer. 15 mg of sample was heated from room temperature to 1000 °C using a heating rate of 10 °C/min and a nitrogen gas (N2) flow rate of 100 mL/min. Resulting TGA curves were analyzed using Advantage TGA software. Textural properties were determined by nitrogen adsorption at 77 K using a Quantachrome instrument (NOVAtouch NT 2LX-1, Volts 220) operated with Quantachrome TouchWin Software Version: 1.22, and surface areas were calculated using the Brunauer–Emmett–Teller (BET) method where, prior to analysis, samples were degassed at 110 °C for 10 h.

3. Results and discussion

3.1. Viability of eggshells as a $CaCO_3$ source

FTIR spectra, Fig. 1, depict that both eggshell powder and

Table 1

Synthetic parameters employed per sample.

| Sample	Reaction Temperature (°C)	Reaction Time (h)	H$_2$O Volume (mL)	DMF Volume (mL)	Product Phase	Yield (g)
1	110	48	0.0	38.0	MOF Not Formed	–
2	110	48	5.0	33.0	MOF Not Formed	–
3	110	48	7.6	30.4	Ca-BDC-tric	0.3587
4	110	48	10.2	27.8	Ca-BDC-tric	0.3642
5	130	72	7.6	30.4	Ca-BDC-tric	0.3590
6	130	72	10.2	27.8	Ca-BDC-tric	0.3673
7	130	48	7.6	30.4	Phase Mixture	0.3621
8	150	48	7.6	30.4	Ca-BDC-orth	0.3589

commercial CaCO$_3$ produce FTIR signals at 711, 871 and 1550–1350 cm^{-1}, ascribed to the in-plane bending vibration, out-of-plane bending vibration and asymmetric stretching of the carbonate ion (CO$_3^{2-}$) in CaCO$_3$ respectively [21]. Theoretical PXRD peaks of commercial CaCO$_3$ occur at 23.2, 29.8, 36.3, 39.7, 43.3, 47.8 and 48.9° on the 2θ scale [20]. The PXRD pattern of eggshells, Fig. 2, exhibits PXRD peaks exclusively at these exact 2θ angles. Thus, PXRD and FTIR spectroscopic analysis confirmed the high CaCO$_3$ content of eggshells and absence of crystalline impurities in eggshell powder.

3.2. Solvent volume optimizations

Various H$_2$O volumes were investigated in the modulator-free synthesis of eggshell-derived Ca(BDC)(DMF)(H$_2$O) at 110 °C for 48 h. Reduction of H$_2$O volume to 0.0 mL (38.0 mL DMF; sample 1) produced a PXRD pattern identical to that of eggshell powder, Fig. 2, indicating that the absence of H$_2$O inhibits Ca(BDC)(DMF)(H$_2$O) synthesis, resulting in zero Ca(BDC)(DMF)(H$_2$O) product formation. Hence, H$_2$O is essential for Ca(BDC)(DMF)(H$_2$O) synthesis, which is substantiated by FTIR spectroscopic analysis, Fig. 1, where the FTIR spectrum of sample 1 exclusively exhibits the three CO$_3^{2-}$ FTIR signals of unreacted CaCO$_3$. Fig. 1 depicts the PXRD pattern calculated from the crystal structure deposited by Mazaj and Logar [17] for Ca-BDC-tric derived from commercial Ca(NO$_3$)$_2$, with main PXRD peaks indexed at 8.3, 9.9 and 10.6° on the 2θ scale. These three PXRD peaks will be used to identify Ca-BDC-tric in further discussions, owing to the unreacted eggshell CaCO$_3$ PXRD peaks that arose amid sample PXRD patterns during solvent volume optimizations in this study. When utilizing a 5.0 mL H$_2$O volume (33.0 mL DMF; sample 2) in the work-up of Ca(BDC)(DMF)(H$_2$O), a PXRD pattern was generated that is almost identical to that of unreacted eggshells, except for the slight emergence of Ca-BDC-tric PXRD peaks at 9.9 and 10.6°, Fig. 2. The intensity of these Ca-BDC-tric PXRD peaks is miniscule relative to the unreacted eggshell CaCO$_3$ PXRD peak at 29.8°,
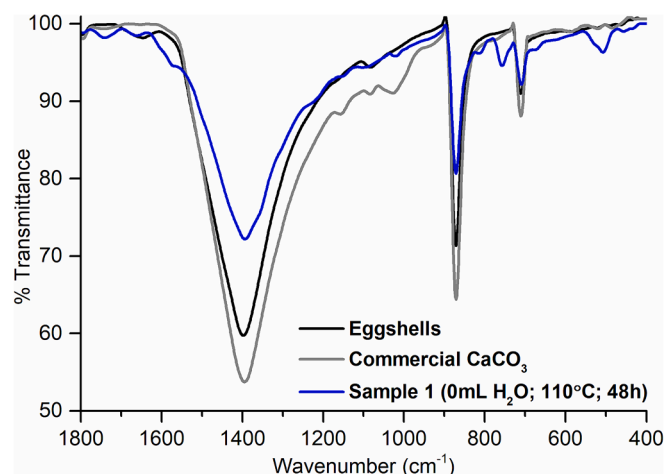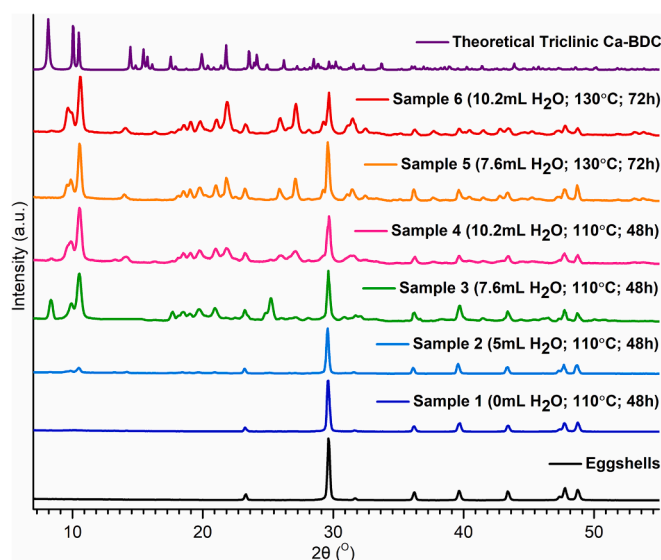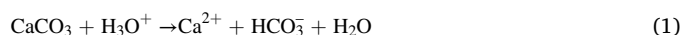

Fig. 2. PXRD patterns of unreacted eggshells and samples prepared using various H$_2$O volumes synthesized at 110 °C for 48 h.

thereby indicating ineffective conversion of eggshell reactant to Ca(BDC)(DMF)(H$_2$O) product when 5.0 mL H$_2$O is used. 7.6 mL (30.4 mL DMF; sample 3) is concluded to be the minimum H$_2$O volume threshold for successful Ca(BDC)(DMF)(H$_2$O) synthesis, where the corresponding PXRD pattern reveals Ca-BDC-tric PXRD peaks at 9.9 and 10.6° with relative intensity almost equal to that of the unreacted eggshell CaCO$_3$ PXRD peak at 29.8°, Fig. 2, signifying an improved Ca-BDC-tric yield. Ca-BDC-tric formation is further increased when 10.2 mL of H$_2$O (27.8 mL DMF; sample 4) was used, where the relative intensity of Ca-BDC-tric PXRD peaks at 9.9 and 10.6° exceed that of the unreacted eggshell CaCO$_3$ PXRD peak at 29.8°, Fig. 2. The use of 10.2 mL H$_2$O (sample 4) produced a 0.3642 g yield of eggshell-derived Ca-BDC-tric, comparable to the 0.3720 g yield obtained when synthesizing Ca-BDC-tric from commercial CaCO$_3$. The advantageous effect of increased H$_2$O volume is not exclusive to a 48 h reaction time or a 110 °C reaction temperature, as used for samples 1-4, as the same trend is evident when subjecting samples to 130 °C for 72 h, samples 5–6, Fig. 2. Therefore, solvent volume optimizations concluded that increasing the H$_2$O volume above 7.6 mL is beneficial as it both enhances Ca-BDC-tric product formation and permits a greener synthesis due to reduction of toxic DMF. The elevated Ca-BDC-tric yield and associated reduction in residual eggshell CaCO$_3$ is explained by the calcium cation (Ca^{2+}) being tied up in eggshell CaCO$_3$ from which it needs to be released before incorporation into the Ca(BDC)(DMF)(H$_2$O) structural framework· H$_2$O is amphiprotic and reacts with CaCO$_3$ as either an acidic or neutral species to liberate Ca^{2+}, eq. 1 and 2 respectively, thereby increasing the Ca^{2+} metal center's concentration in solution.

$$CaCO_3 + H_3O^+ \rightarrow Ca^{2+} + HCO_3^- + H_2O \qquad (1)$$

Fig. 1. FTIR spectra of unreacted eggshells, commercial CaCO$_3$ and sample 1.

$$CaCO_3 + H_2O \rightarrow Ca^{2+} + HCO_3^- + OH^- \qquad (2)$$

The minimum 7.6 mL H_2O volume threshold is further confirmed by the emergence of characteristic $Ca(BDC)(DMF)(H_2O)$ FTIR signals when H_2O volumes at and above 7.6 mL are used, Fig. 3. Specifically, the most obvious indication of successful $Ca(BDC)(DMF)(H_2O)$ formation is the calcium-oxide (Ca-O) signal at 500 cm^{-1}, Fig. 3, indicating successful formation of CaO_8 polyhedra [19]. The Ca-O FTIR signal is present when 7.6 mL H_2O is used (samples 3, 7 and 8; Fig. 3) but absent in samples prepared using H_2O volumes less than 7.6 mL, Fig. 1. Additionally, successful coordination of the BDC linker to Ca^{2+} metal centers is indicated by FTIR signals at 1665 and 1560 cm^{-1} respectively, Fig. 3, ascribed to the symmetric and asymmetric vibration of coordinated carboxylate (COO$^-$) respectively [17]. These FTIR signals confirm the loss of an acidic proton (H$^+$) from the carboxylic acid group (COOH) of terephthalic acid (H_2BDC) for subsequent coordination in the $Ca(BDC)(DMF)(H_2O)$ structural framework [17].

3.3. Temperature phase study

Reaction temperatures of 80 °C and 150 °C were investigated for Ca(BDC)(DMF)(H_2O) derived from commercial calcium salts by Mazaj and Logar [17], whereas this study provides insight on the relative phase prevalence of eggshell-derived Ca-BDC-tric and Ca-BDC-orth when adopting temperatures between 110 °C and 150 °C. The PXRD pattern calculated from the crystal structure deposited by Mazaj and Logar [17] for Ca-BDC-orth derived from commercial Ca(NO$_3$)$_2$ is available in Fig. 5, with PXRD peaks indexed at 9.6, 21.9, 25.9, 27.1 and 29.3° on the 2θ scale. The effect of three reaction temperatures (110, 130 and 150 °C) on eggshell-derived Ca(BDC)(DMF)(H_2O) were investigated using a long 48 h reaction time to ensure complete reaction of eggshell precursors. Ca-BDC-tric was obtained at 110 °C (sample 3) and exhibited PXRD peaks at 8.3, 9.9 and 10.6°, Fig. 4, with corresponding Ca-BDC-tric hkl indices in Table 2. Ca-BDC-orth, with associated hkl indices in Table 2, was obtained at 150 °C, sample 8, producing PXRD peaks at 9.6, 21.9, 25.9, 27.1 and 29.3°, Fig. 4. A phase mixture prevailed when a 130 °C reaction temperature was employed (sample 7), where the corresponding PXRD pattern exhibits Ca-BDC-orth peaks at 21.9, 25.9, 27.1 and 29.3°, as well as Ca-BDC-tric peaks at 9.9 and 10.6°. This observation explains that Ca-BDC-tric obtained at lower temperatures (110 °C) begins to morph into Ca-BDC-orth at higher temperatures (130 °C). For this reason, Ca-BDC-tric was dried at 110 °C to prevent conversion to Ca-BDC-orth. The SEM image of the phase mixture (sample 7; Fig. 5) confirms the dual-presence of both phases, depicting orthorhombic rods dispersed among triclinic crystals. Ca-BDC-orth (150 °C) manifests as a rod-like morphology, whereas the morphology of Ca-BDC-tric (110 °C) resembles flower-like aggregates, Fig. 5. It was observed that increasing
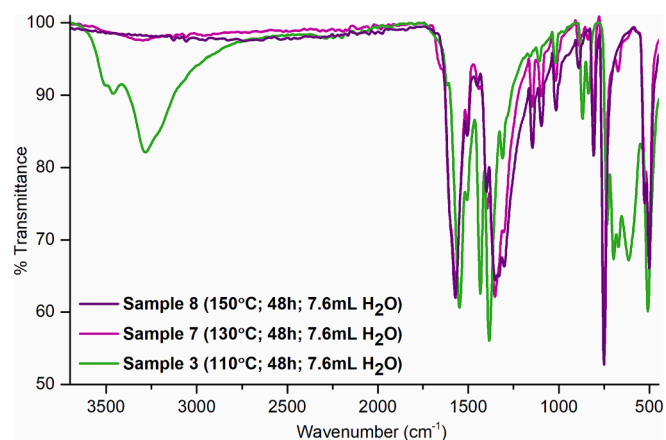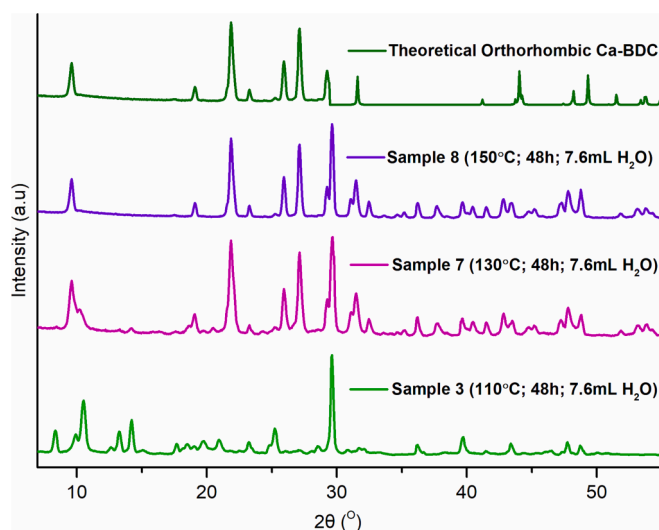
Fig. 4. PXRD patterns of eggshell-derived Ca(BDC)(DMF)(H_2O) synthesized at various reaction temperatures for 48 h.

Table 2
hkl indices for eggshell-derived Ca-BDC-tric and Ca-BDC-orth.

Ca(BDC)(DMF)(H_2O) Phase	2θ Degree	hkl indices
Triclinic	8.30	1,0,0
	9.87	0,1,0
	10.58	1,1,0
Orthorhombic	9.62	2,0,0
	21.85	1,1,-1
	27.13	2,0,2

solvothermal temperature promotes Ca-BDC-orth formation and, thereby elevates its abundance relative to Ca-BDC-tric until it is, ultimately, synthesized in entirety at 150 °C. This observation is substantiated by the intensity increase of the Ca-BDC-orth PXRD peak at 21.9°, relative to the unreacted CaCO$_3$ peak at 29.8°, when moving from a lower temperature (110 °C; sample 3) to a higher temperature (150 °C; sample 8), Fig. 4. The similarity between PXRD patterns of eggshell-derived Ca(BDC)(DMF)(H_2O), reported in this study, and those presented in previous literature [17] indicates that substitution of commercial calcium salts with eggshell CaCO$_3$ retains correct Ca(BDC)(DMF)(H_2O) crystal structure. The only discrepancy between literature PXRD patterns and those of this study are the unreacted eggshell CaCO$_3$ peaks amid Ca(BDC)(DMF)(H_2O) PXRD patterns at 23.2, 29.8, 36.3, 39.7, 43.3, 47.8 and 48.9°, Figs. 2 and 4, attributable to the absence of a modulator in this study's green solvothermal synthesis that relied solely on the amphiprotic nature of H_2O to acidify eggshell CaCO$_3$.

3.4. Structure and porosity

In both phases, Ca(BDC)(DMF)(H_2O) consists of edge-sharing CaO$_8$ polyhedra that form continuous chains [17]. Polyhedra are distorted bicapped prisms with eight-fold coordinated cationic calcium metal centers (Ca^{2+}) that coordinate to six oxygen atoms of 1,4-benzenedicarboxylic acid (BDC), one of N,N-dimethylformamide (DMF) and one of H_2O. Ca-BDC-orth and Ca-BD-tric crystallize as similar yet distinguishable structural frameworks. In both phases, the carbonyl (C=O) bond of coordinated DMF is delocalized, causing the DMF molecule to be mostly planar [17]. In Ca-BDC-tric (110 °C; sample 3), planar DMF molecules are orientated parallel to channel direction, enabling a porous phase capable of H_2O adsorption [17]. Successful formation of Ca-BDC-tric (110 °C) is confirmed by FTIR spectra, where Ca-BDC-tric produced FTIR signals at 3510 cm and 3280 cm^{-1}, Fig. 3, ascribed to the

Fig. 3. FTIR spectra of eggshell-derived Ca(BDC)(DMF)(H_2O) synthesized at various reaction temperatures for 48 h.
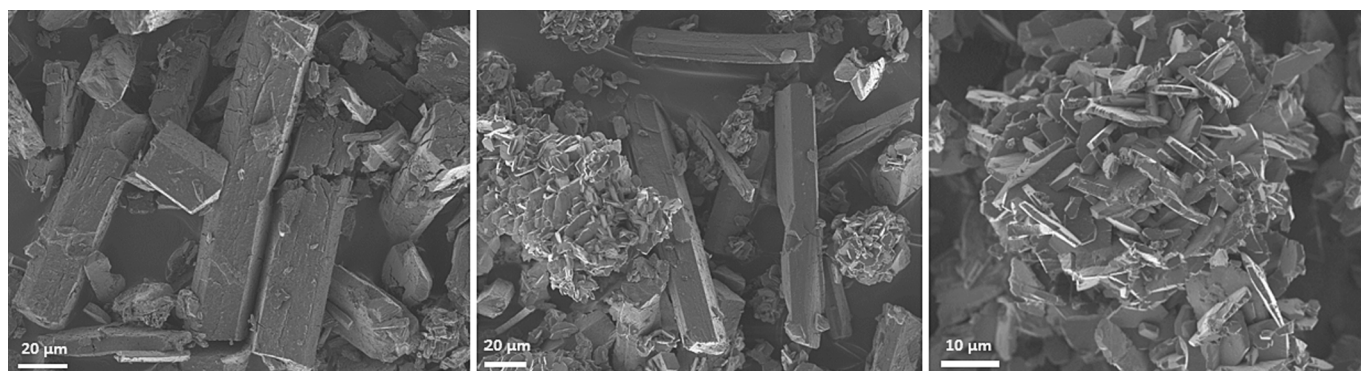
Fig. 5. SEM images of eggshell-derived: Ca-BDC-orth (sample 8; left), phase mixture (sample 7; middle) and Ca-BDC-tric (sample 4; right).

asymmetric and symmetric stretch of coordinated H_2O molecules respectively, as well as a signal at 3465 cm^{-1}, attributable to adsorbed H_2O [17]. Ca-BDC-tric porosity was also confirmed by sorption analysis, where Ca-BDC-tric (sample 4) generated the largest V_{pore} of the two phases (0.0379 cm^3.g^{-1}; Table 3), which exceeds literature Ca-BDC-tric V_{pore} values (0.035 cm^3.g^{-1}) [19]. Similarly, Ca-BDC-tric (sample 4) also produced the largest surface area (S_{BET}) of the two phases (13.669 m^2.g^{-1}; Table 3). Conversely, DMF molecules are positioned perpendicular to channel direction in Ca-BDC-orth (150 °C), resulting in complete blocking of pores [17]. Hence, Ca-BDC-orth pores are inaccessible to guest molecules, explaining the absence of adsorbed H_2O FTIR signals, Fig. 3. Accordingly, Ca-BDC-orth (sample 8) produced the smallest V_{pore} and S_{BET} of 0.0020 cm^3.g^{-1} and 0.667 m^2.g^{-1} respectively, Table 3. The phase mixture (130 °C; sample 7) produced V_{pore} (0.0187 cm^3.g^{-1}) and S_{BET} (6.569 m^2.g^{-1}) values intermediate to those obtained for Ca-BDC-tric and Ca-BDC-orth, Table 3. Therefore, substitution of commercial calcium salts with eggshells in the workup of Ca(BDC)(DMF)(H_2O) upholds that Ca-BDC-tric and Ca-BDC-orth are porous and non-porous phases respectively.

3.5. Thermal decomposition

Ca-BDC-tric (110 °C; sample 4) exhibited a 5% weight loss up until roughly 150 °C, ascribed to the evaporation of H_2O adsorbed within accessible pores, Fig. 6. Conversely, Ca-BDC-orth (150 °C; sample 8) exhibits no weight loss in this temperature region, attributable to pore-blocking by perpendicularly-orientated DMF molecules, inhibiting H_2O adsorption. A 4% weight loss was also observed for the phase mixture (130 °C; sample 7) confirming the presence of Ca-BDC-tric alongside Ca-BDC-orth. Considering both phases were dried at 110 °C to prevent Ca-BDC-tric from morphing into Ca-BDC-orth, evaporation of surface DMF solvent occurs between 120 °C and 400 °C in both phases, Fig. 6. Weight loss after 500 °C occurs due to decomposition of BDC linkers and co-ordinated DMF, causing degradation of the Ca(BDC)(DMF)(H_2O) structural framework. Therefore, both phases of eggshell-derived Ca(BDC)(DMF)(H_2O) exhibit thermal stability up to roughly 500 °C, the temperature at which BDC linkers and coordinated DMF are removed, exceeding thermal stability of Ca(BDC)(DMF)(H_2O) synthesized from commercial $CaCO_3$ in literature (450 °C) [19]. The final solid metal

Fig. 6. TGA curves of eggshell-derived Ca(BDC)(DMF)(H_2O) synthesized at various reaction temperatures for 48 h..

oxide (CaO) is formed at 800 °C.

4. Conclusion

This study successfully devised a modulator-free solvothermal synthetic method for the four-component eggshell-derived Ca(BDC)(DMF)(H_2O) MOF. In doing so, this study eliminated the need for energy-intensive processes that convert limestone, dolomite and aragonite into commercial $CaCO_3$ by use of eggshells directly as a precursor, whilst also improving atom economy by elimination of a modulator. Eggshell-derived Ca(BDC)(DMF)(H_2O) synthesis was optimized by increasing the H_2O volume relative to DMF to promote liberation of Ca^{2+} from eggshell $CaCO_3$, where increasing the H_2O volume above the 7.6 mL minimum H_2O volume threshold enhanced Ca-BDC-tric yield. Phase investigations were conducted at long reaction times to prevent the effect of reaction times from perturbing phase study results. The effect of reaction temperature played no role in optimization but, instead, determined the predominant Ca(BDC)(DMF)(H_2O) phase. Optimal synthetic parameters for exclusive formation of Ca-BDC-tric were 10.2 mL H_2O, 110 °C and 48 h. Synthetic conditions for Ca-BDC-orth were 7.6 mL H_2O, 150 °C and 48 h, where high temperatures (150 °C) were crucial to avoid the phase mixture that prevailed at 130 °C. The substitution of commercial calcium salts with an eggshell precursor in the workup of Ca(BDC)(DMF)(H_2O) produced Ca(BDC)(DMF)(H_2O) with thermal stability and V_{pore} exceeding that in literature.

CRediT authorship contribution statement

Gizelle R. van Niekerk: Methodology, Investigation, Validation, Visualization, Writing – original draft. **Henrietta W. Langmi:**

Table 3
Influence of reaction temperature on eggshell-derived Ca(BDC)(DMF)(H_2O) phase and textural properties.

Sample	Reaction Temperature (°C)	Ca(BDC)(DMF)(H_2O) Phase	V_{pore} (cm^3.g^{-1})	S_{BET} (m^2.g^{-1})
4	110	Triclinic	0.0379	13.669
7	130	Phase Mixture	0.0187	6.569
8	150	Orthorhombic	0.0020	0.667

Conceptualization, Methodology, Resources, Supervision, Funding acquisition, Writing – review & editing.

Declaration of Competing Interest

The authors declare that they have no known competing financial interests or personal relationships that could have appeared to influence the work reported in this paper.

Data availability

Data will be made available on request.

Acknowledgements

References

[1] H. Forbes, T. Quested, C. O'Connor C, Food Waste Index Report 2021, United Nations Environment Programme, 2021 https://www.unep.org/resources/report/unep-food-waste-index-report-2021 (accessed 14 September 2022).

[2] M. Waheed, M. Yousaf, A. Shehzad, M. Inam-Ur-Raheem, M.K.I. Khan, M.R. Khan, N. Ahmad, Abdullah, and, R.M., Aadil,, Channelling Eggshell Waste to Valuable and Utilizable Products: A Comprehensive Review, Trends Food Sci. Technol. 106 (2020) 78–90, https://doi.org/10.1016/j.tifs.2020.10.009.

[3] S. Ray, A.K. Barman, P.K. Roy, B.K. Singh, Chicken Eggshell Powder as Dietary Calcium Source in Chocolate Cakes, J. Pharm. Innov. 9 (2017) 1–4.

[4] S. Polat, P. Sayan, Ultrasonic-Assisted Eggshell Extract-Mediated Polymorphic Transformation of Calcium Carbonate, Ultrason. Sonochem. 66 (2020) 1–11, https://doi.org/10.1016/j.ultsonch.2020.105093.

[5] I. Abdulrahman H.I. Tijani B.A. Mohammed H. Saidu H. Yusuf M. Ndejiko Jibrin S. Mohammed From Garbage to Biomaterials: an Overview on Eggshell Based Hydroxyapatite J. Mater. 2014 2014 1 6 e802467.

[6] M. Hyman, M,, Guidelines for National Waste Management Strategies: Moving from Challenges to Opportunities, accessed 16 September 2022, United Nations Environment Programme (2013), https://www.unep.org/ietc/resources/toolkits-manuals-and-guides/guidelines-national-waste-management-strategies-moving.

[7] S. Kaza, L.C. Yao, P. Bhada-Tata, F. Van Woerden, What a Waste 2.0: A Global Snapshot of Solid Waste Management to 2050, World Bank, 2018 accessed 15 September 2022.

[8] E.O. Ajala, O.A.A. Eletta, M.A. Ajala, S.K. Oyeniyi, Characterization and Evaluation of Chicken Eggshell for Use as a Bio-Resource, Arid Zone J. Eng. Technol. Environ. 14 (2018) 26–40.

[9] S.C. Onwubu, A. Vahed, S. Singh, K.M. Kanny, Reducing the Surface Roughness of Dental Acrylic Resins by Using an Eggshell Abrasive Material, J. Prosthet. Dent. 117 (2017) 310–314, https://doi.org/10.1016/j.prosdent.2016.06.024.

[10] M. Gaonkar, A.P. Chakraborty, Application of Eggshell as Fertilizer and Calcium Supplement Tablet, Int. J. Innov. Res. Technol. Sci. Eng. 5 (2016) 3520–3525, https://doi.org/10.15680/IJIRSET.2016.0503183.

[11] P. Kamalanathan, S. Ramesh, L.T. Bang, A. Niakan, C.Y. Tan, J. Purbolaksono, H. Chandran, W.D. Teng, Synthesis and Sintering of Hydroxyapatite Derived from Eggshells as a Calcium Precursor, Ceramics Int. 40 (2014) 16349–16359, https://doi.org/10.1016/j.ceramint.2014.07.074.

[12] Y.K. Lee, A.Y. Kim, S.G. Min, H.S. Kwak, Characteristics of Milk Tablets Supplemented with Nanopowdered Eggshell or Oyster Shell, Int. J. Dairy Technol. 69 (2016) 337–345, https://doi.org/10.1111/1471-0307.12268.

[13] H. Daraei, A. Mittal, M. Noorisepehr, J. Mittal, Separation of Chromium from Water Samples Using Eggshell Powder as a Low-Cost Sorbent: Kinetic and Thermodynamic Studies, Desalination, Water Treat. 53 (2015) 214–220, https://doi.org/10.1080/19443994.2013.837011.

[14] A.M. Muliwa, T.Y. Leswifi, M.S. Onyango, Performance Evaluation of Eggshell Waste Material for Remediation of Acid Mine Drainage from Coal Dump Leachate, Miner. Eng. 122 (2018) 241–250, https://doi.org/10.1016/j.mineng.2018.04.009.

[15] M. Ding, R.W. Flaig, H. Jiang, O.M. Yaghi, Carbon Capture and Conversion Using Metal-Organic Frameworks and MOF-Based Materials, Chem. Soc. Rev. 48 (2019) 2783–2828, https://doi.org/10.1039/C8CS00829A.

[16] S. Xian, Y. Lin, H. Wang, J. Li, Calcium-Based Metal-Organic Frameworks and their Potential Applications, Nano, Micro, Small. 17 (22) (2021).

[17] M. Mazaj, N.Z. Logar, Phase Formation Study of Ca-Terephthalate MOF-Type Materials, Cryst. Growth Des. 15 (2015) 617–624, https://doi.org/10.1021/cg501273b.

[18] P. Po-Hsueh Chang, H. Hsu, S. Wu, C. Peng, Synthesis and Formation Mechanism of Limestone-Derived Porous Rod Hierarchical Ca-based Metal-Organic Framework for Efficient CO2 Capture, Materials. 13 (2020) e4297.

[19] U. Jamil, A.H. Khoja, R. Liaquat, S.R. Naqvi, W.N.N.W. Omar, N.A.S. Amin, Copper and calcium-based metal organic framework (MOF) catalyst for biodiesel production from waste cooking oil: A process optimization study, Energy Convers. Manag. 215 (2020) e112934.

[20] T.S. Crickmore, H.B. Sana, H. Mitchell, M. Clark, D. Bradshaw, Toward sustainable syntheses of Ca-based MOFs, Chem. Commun. 57 (2021) 10592–10595, https://doi.org/10.1039/D1CC04032D.

[21] S. Veerasingam, R. Venkatachalapathy, Estimation of carbonate concentration and characterization of marine sediments by Fourier Transform Infrared Spectroscopy, Infrared Phys. Technol. 66 (2014) 136–140, https://doi.org/10.1016/j.infrared.2014.06.005.